



PERGAMON

Aerosol Science 33 (2002) 595–608

Journal of
Aerosol Science

www.elsevier.com/locate/jaerosci

Number and sulfur derived 3-parameter aerosol size distributions in the tropopause region from CARIBIC flights between Germany and the Indic

Jost Heintzenberg^{a,*}, Markus Hermann^a, Bengt G. Martinsson^b,
Giorgos Papaspiropoulos^b

^a*Institute for Tropospheric Research, Permoserstrasse 15, 04303 Leipzig, Germany*

^b*Division of Nuclear Physics, Lund University, 22100 Lund, Sweden*

Received 19 July 2001; accepted 29 October 2001

Abstract

Aerosol number concentrations in three size ranges ($d_p > 4$, $d_p > 12$, $18 \leq d_p \leq 135$ nm) and sulfur mass from impactor samples were collected over a total of about 120 sampling hours on 18 long-range commercial flights between the northern mid-latitudes and the equatorial region covering an altitude range between 8.8 and 11.2 km. The data were evaluated with a new random search algorithm to derive monomodal lognormal particle size distributions. Through tests of the algorithm using synthetic data and size distributions from mountain stations the retrieval capabilities of the fitting algorithm are established.

The fitting of aerosol data yields three parameters of the submicrometer size distribution. Their latitudinal trends indicate the influence of tropical and mid-latitudinal source regions on the tropopause aerosol. Total particle numbers show maxima near tropical biomass burning and over the European regions. Geometric mean diameters decrease north of 35°N while the width of the distribution increases, indicating a move towards more frequent recent nucleation events or more frequent bimodal size distributions. © 2002 Elsevier Science Ltd. All rights reserved.

1. Introduction

Aerosol properties in the upper troposphere and lower stratosphere (UT/LS) are still the least constrained by experimental findings as compared to other lower atmospheric regions. The origin of the particles in the UT/LS can be attributed to transport, local primary emissions, or the local formation of new particles by gas to particle conversion from condensable precursors.

* Corresponding author. Tel.: +49-341-235-2321; fax: +49-341-235-2361.

E-mail address: jost@tropos.de (J. Heintzenberg).

In the tropics, deep convective transport carries particles into the upper troposphere, whereby the majority of particle volume is removed by wet scavenging processes. Although less frequent, recent measurements indicate that also at midlatitudes large scale and convective transport is responsible for high particle concentrations in the tropopause region (Hermann, 2000; Wang et al., 2000). Single, larger natural events, like volcanic activities (Hofmann, 1993) or biomass burning (Crutzen & Andreae, 1990; Hofmann, 1993), can likewise contribute to upper tropospheric particles.

The only direct anthropogenic source for particles in the upper troposphere are aircraft exhausts, which are concentrated at northern mid-latitudes. This source deserves particular attention because world-wide civil aviation traffic is growing exponentially, currently 5–6% per year (Brasseur et al., 1998). Primary aircraft-emitted particles consist mainly of soot. Their size distribution can be described by a monomodal lognormal distribution between 15 and 200 nm, peaking at 30–60 nm.

Besides primary particles, deep convection in the tropics carries also particle precursor gases from the surface to higher altitudes. These gases are oxidized during transport and contribute to homogeneous particle nucleation yielding mainly sulfuric acid/water particles (Brock, Hamill, Wilson, Jonsson, & Chan, 1995; Clarke, 1993), but also other condensable species can be found. Furthermore, aircraft engines are a source of sulfuric acid particles, which result from the oxidation of fuel sulfur to SO₂ and H₂SO₄ with subsequent gas to particle conversion.

In general, particle number concentrations decrease with increasing altitude from values of about 200–20 000 particles cm⁻³ in the boundary layer to a few hundred particles cm⁻³ (ambient) in the free troposphere (Jaenicke, 1992). However, several groups observed a secondary maximum in particle number concentration, just below the tropopause (Brock et al., 1995; de Reus et al., 1998; Hagen, Podzimek, & Trueblood, 1995; Hofmann, 1993; Schröder & Ström, 1997).

In the stratosphere, particle number concentrations are rather low, mostly below 100 cm⁻³ (ambient). Furthermore, very low ultrafine particle concentrations suggest that particle nucleation in the stratosphere is quite rare. Both facts indicate a rather aged aerosol in the mid-latitude stratosphere, which corresponds to the mean meridional stratospheric circulation (Hamill, Jensen, Russell, & Bauman, 1997).

Particle number concentrations for the mid-latitude troposphere are more variable compared to the stratosphere and range between 500 and 5000 cm⁻³ STP in the majority of cases (Hermann, 2000). Ultrafine particle concentrations can reach high values (> 5000 cm⁻³ STP), indicating recent new particle formation. Tropical particle number concentrations are very high (Hermann, 2000). They can be explained by particle formation processes in the upper tropical troposphere.

Measurements of the particle size distribution in the upper troposphere, which cover the whole submicrometer size range, are very rare and because of sampling problems not always reliable. Over Europe most data with instrumentation comparable to the CARIBIC payload have been derived onboard of the German research aircraft Falcon (Schröder et al., 2000; Schröder & Ström, 1997; Schröder, 2000). A somewhat typical distribution as determined at 5–6 km altitude with a diffusion battery (Zaizen et al., 1996) shows the number dominating peak between 20 and 100 nm, comparable to size distributions in surface sink areas such as the boreal Arctic (Heintzenberg & Covert, 1987) and austral winter Antarctic (Ito, 1993). Distributions at higher altitudes look similar (Hagen et al., 1995; Poeschel, Livingston, Ferry, & De Felice, 1994; Schröder & Ström, 1997).

Aerosol particles in the UT/LS can contain many chemical compounds (Murphy, Thompson, & Mahoney, 1998). However, most of the time the chemical composition of particles is dominated by only a few substances, mostly sulfates (Sheridan, Brock, & Wilson, 1994; Yamato & Ono, 1989) and organics (Murphy et al., 1998).

Amongst other goals the CARIBIC research project (Brenninkmeijer et al., 1999) was designed to increase systematically the very limited knowledge of the UT/LS aerosol as summarized above. Beginning in 1999 on long-range commercial flights continuous measurements of particle number concentrations in three size ranges are taken together with particle samples for subsequent laboratory analyses.

A statistical discussion of the particle number concentrations has been presented in Hermann et al. (2001a). The sulfur data from the first CARIBIC flights with an automated particle sampler have been discussed in Martinsson, Papaspiropoulos, Heintzenberg, and Hermann (2001). In the present study, we explore the possibilities of combining the physical and chemical CARIBIC data to deduce parameters of the UT/LS sub-micrometer size distribution by a random search algorithm. The fitting results will be analyzed in terms of latitudinal distributions and statistical relationships between the size distribution parameters in this largely uncharted part of the atmosphere.

2. Experimental

Particle number concentrations used in this study were measured with a combination of three condensation particle counters (CPCs, TSI Model 7610, St. Paul, MN) operated in parallel. These instruments have been modified for low-pressure conditions and aviation requirements, and were extensively tested with respect to their counting efficiency at operating pressures of 160–1000 hPa (Hermann & Wiedensohler, 2001). The lower threshold diameters of the CPCs (i.e. the particle diameter with 50% detection efficiency) were set to 4 nm (CPC1), 12 nm (CPC2), and 18 nm (CPC3), respectively, by increasing or decreasing the temperature difference between the saturator and condenser block inside the counters. To restrict the size range of CPC3 to Aitken particles, a pre-impactor with a pressure and temperature dependent 50% transmission diameter of about 135 nm was mounted upstream of this counter (Hermann, 2000).

Besides the CPCs, a particle sampler was used to collect particles for elemental analysis. This instrument consists of 14 identical impactors with a threshold diameter of approximately 65 nm at flight level pressures (Papaspiropoulos, Mentes, Kristiansson, & Martinsson, 1999). Each CARIBIC flight mission consisted of one outbound and one return flight to the home airport in Germany with no payload service in between. Thus, with the high number of impactors both flights of one mission could be covered. During flight, impactors are opened sequentially for 1–3 h depositing particles larger than the threshold diameter on thin (0.1 μm), high-purity polyimide films (AP1TM), which exhibit superior properties with respect to analytical detection limits compared to traditional aerosol sampling substrates. On ground, the sampled particle mass is analyzed for elemental chemical composition by PIXE analysis (Malmqvist, 1984). In flight, CPC data were recorded with a time resolution of 2 s. For the present study the primary CPC data were averaged over 1 min before using them in connection with the chemical analyzes from the particle sampler, i.e. before averaging them further over the specific time periods of the impactor samples.

The CPCs and the particle sampler are mounted together with trace gas instruments in a modified standard airfreight container. This container is flown regularly aboard a commercial aircraft (B 767-300 ER, LTU International Airways) within the scope of the CARIBIC project (Brenninkmeijer et al., 1999). For collection and transport of sample air from outside the aircraft to the container in the cargo compartment a dedicated aerosol and trace gas inlet is mounted on the aircraft fuselage directly below the container. The sampling efficiency of this inlet including line losses between the inlet and the individual sensors and the samplers has been characterized by calculations and wind tunnel experiments (Hermann, Stratmann, Wilck, & Wiedensohler, 2001b).

In the literature, particle concentrations are given in various quantities and units. In this study, all particle data are given as concentrations per cubic centimeter or cubic meter, converted to standard conditions (STP: 1013.25 hPa and 273.15 K).

3. Primary results

The present data set was collected over the period March 26, 1999–April 14, 2000 on 18 flights between Germany and the Indic (Colombo, Sri Lanka or Male, Maldives). For the analysis, only data from level flight sections were used on altitudes between 3500 and 11900 m a.s.l. Sample-averaged altitudes were between 8800 and 11200 m a.s.l. The 1 min resolution CPC data were averaged over the 51 sampling periods of the PIXE impactor which lasted between two and three hours (median 2.4 h). Each of these 51 periods comprises one sample or one data set for the inversion in the following text.

For the present fitting purpose the CPC data were corrected for coincidence errors and normalized to STP conditions. Line losses, size, temperature, and pressure-dependent collection efficiencies were taken into account in detail as part of the fitting algorithm.

An overview of the total data set of the present investigation can be found on (www.caribic-atmospheric.com/). It includes sample average concentrations and standard deviations of the three CPCs, sulfur concentrations, geographical start and stop positions of the samples, ambient pressure, and temperature during the samples. Here the standard deviations were taken of the individual 1 min CPC data over the respective sampling periods. Number concentrations scattered over the range 10^3 – 10^4 cm⁻³ STP with a few excursions beyond 10^4 cm⁻³, indicating influence from recent particle nucleation (Schröder & Ström, 1997; Schröder et al., 1998; Ström, Fischer, Lelieveld, & Schröder, 1999), possibly prior to rapid convective transport to the sampling altitudes.

Sulfur mass concentrations in the PIXE samples ranged between 1 and 100 ng m⁻³ STP. On these samples sulfur was either the only detected element or by far the mass dominating one (Martinsson et al., 2001). In accord with many chemical studies of the UT/LS aerosol we consequently assumed that (a) sulfur was the mass-controlling element and (b) that all sulfur existed in the form of sulfate (Brock et al., 1995; Ferry et al., 1999; Sheridan et al., 1994; Yamato & Ono, 1989). The effects of this grave assumption on the fitting results is reflected by the large uncertainties that are allowed in the algorithm for the fitting of the PIXE-data (–20–+50%), which are much larger than the experimental uncertainty of the PIXE-data (on the order of 15%). The chosen asymmetrical error bounds thus allow for the possibility that additional unanalyzed particulate mass besides sulfate (e.g., organics) contributed to the samples.

4. Fitting algorithm

Many of the inversion methods that have been developed for the retrieval of atmospheric properties from measurable quantities utilize minimization search algorithms (e.g., Deepak, 1977). When retrieving aerosol size distributions different model assumptions concerning the shape of the distributions have been made, e.g., histograms (Heintzenberg, 1978), gamma distributions (Tampieri & Tomasi, 1976), or lognormal functions (Birmili, Wiedensohler, Heintzenberg, & Lehmann, 2001; Puttock, 1981). In the latter case, frequently high-resolution number size distributions are being reduced in terms of the number of the distribution parameters to one or several lognormal distributions, the integral parameters of which are determined. For the lognormal fits various numerical procedures have been applied, often simple numerical tools that come with commercial software such as spreadsheet applications.

In the present case the retrieval proceeds in the opposite direction by utilizing measured integral properties of the aerosol size distribution to derive size distribution parameters, an approach that has been utilized by others with various types of algorithms (e.g., Heintzenberg, 1975; Shifrin & Kolmakkov, 1967; Sverdrup & Whitby, 1977; Wright 2000 Wright Jr., 2000). For the joint evaluation of CPC and PIXE data a fitting algorithm was formulated that fits one lognormal size distribution to any measured data set. A data set consists of three partial integrals of the number distribution (3 CPC channels) and one partial integral over the mass distribution (PIXE-SO₄). All four integrals need to be calculated accounting for the respective sampling efficiencies, which are pressure and temperature dependent and thus are evaluated separately for each individual sample. In the case of the PIXE samples only the diameters of 50% collection efficiency were known from calibrations. We assumed 0% and 100% collection efficiencies 15% below and above the actual 50% collection diameters, respectively. For the calculation of mass concentrations a particle density ρ has to be assumed. For the UT/LS region we assume and use a value of 1.55 g cm^{-3} throughout this study, according to the data given in Tabazadeh, Toon, Clegg, and Hamill (1997) and Krieger, Mossinger, Luo, Weers, and Peter (2000). We assume that the uncertainty of this fixed estimate for the particle density is taken into account by the large error bars allowed for the mass data in the fitting algorithm. Fig. 1 shows the size-dependent collection efficiencies of the four instruments combined with sampling and transmission characteristics of the inlet system as they are used in the fitting algorithm to simulate the measured data for a given lognormal size distribution.

From the four measured parameters the three parameters of a lognormal distribution, i.e. total number N , geometric median diameter d_g , and geometric standard deviation σ_g can be determined with e.g., non-linear optimization techniques. However, there is no unique solution to the problem. The large uncertainties (20–50%) in the input parameters exclude the use of conventional numerical techniques such as matrix inversions. Instead, a search algorithm was constructed which picks at random sets of lognormal parameters within given ranges. Because of the large expected dynamic range of particle number and size the logarithms of N and d_g were varied at random. The same was done with the random search of the geometric standard deviation because of its non-linear effect on the fitting results. As one of the partial integrals (CPC1) always is close to the total particle number, the respective input parameter of an input data set was used to determine the search range for N , allowing values from 1/10 to 10 times the respective input value in the search. For d_g a range of 3–50 nm and for σ_g a range of 1.01–5 was allowed.

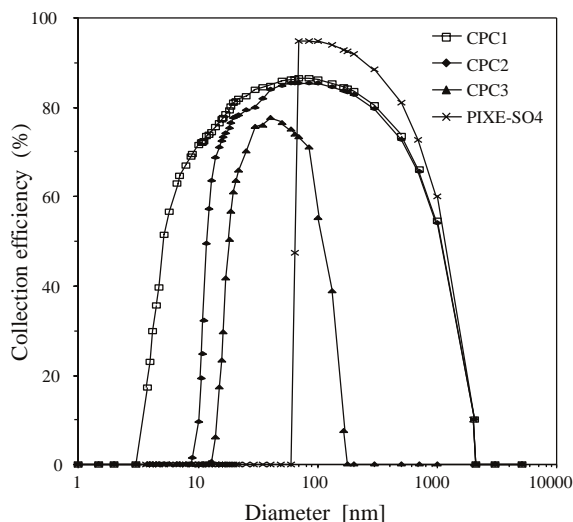


Fig. 1. Collection efficiencies of the four CARIBIC aerosol instruments combined with the efficiencies of inlet and sampling lines. CPC1 = \square , CPC2 = \blacklozenge , CPC3 = \blacktriangle , PIXE-SO4 = \times .

No numerical optimization is applied in the algorithm. Instead, each randomly picked set of lognormal parameters that reproduces the input data within given relative error bounds is accepted. As random number generator the corresponding system routine of the Macintosh system OS8.6 of the present computer is reseeded anew for each inversion trial. For the experimentally determined particle concentrations symmetrical error bounds about a measured value apply ($\approx 20\%$). However, the use of PIXE-SO4 as a proxy for the particulate mass involves additional assumptions, which are taken into account in the algorithm as follows. Below any given PIXE-SO4 value an error of 20% is used, which is somewhat larger than the experimental uncertainty of 15% whereas above this value a higher uncertainty of 50% is allowed, (cf. Section 3), for the acceptance of a fitting solution. As there is no unique optimum solution, the fitted three parameters are reported in terms of median and range of values within which 90% of a given number of solutions are found.

As a numerical test of the quality of the method, synthetic data sets—equivalent to the CARIBIC data sets—are generated for given lognormal distributions. These synthetic data are then fitted with given error bounds of the input parameters. According to our calibration of the combination of inlet, transmission lines, and sensors (Hermann et al., 2001b; Hermann & Wiedensohler, 2001), the experimental data of the CARIBIC experiment cover a diameter range between 5 and about 500 nm. For the test, this range was covered in five diameter octaves from 10 to 320 nm in terms of d_g . For the synthetic data σ_g was varied between 1.5 and 3.5. Obviously, there is no need to vary N in this test.

Fig. 2 gives examples of average fitting solutions for the frequently found value of $\sigma_g = 1.5$. Other values of the geometric standard deviation (not shown here) yield similar results. Over the whole range of d_g (thick solid line) the 90% range of fitted parameters given in Fig. 2 as error bars covers the respective true values. This result holds even for input uncertainties of 30% and 60% for CPCs and PIXE-SO4, respectively (not shown here). When the three CPC data differ from each other by their experimental uncertainty or less, the information content of the experimental data set

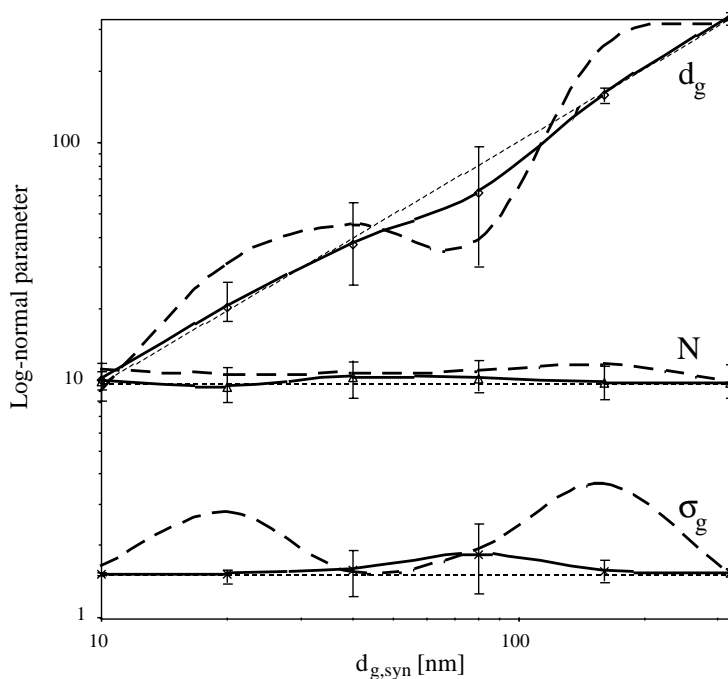


Fig. 2. Fitted lognormal parameters for synthetic CARIBIC data calculated for lognormal number size distributions with total number concentration N of 10 cm^{-3} , geometric standard deviation σ_g of 1.5 and geometric median diameters $d_{g, \text{syn}}$ of 10, 20, 40, 80, 160 and 320 nm. Relative uncertainties of 20% for the CPCs and $-20/+50\%$ for PIXE-SO₄ were allowed in the algorithm. The fitted lognormal parameters N_{inv} , $d_{g, \text{inv}}$, and $\sigma_{g, \text{inv}}$, (solid lines), represent median solutions. 90% of a total of 100 solutions are found within the given error bars. For comparison the synthetic lognormal parameters are shown as thin dashed lines. Median solutions without the information of PIXE-SO₄ are shown as thick dashed lines. All volumetric data refer to STP.

is reduced. Consequently, the largest deviations between input and fitted data occur for these cases. The maximum relative deviations of the median fits from given synthetic lognormal parameters in Fig. 2 are 8%, 24%, and 22% for N , d_g , σ_g , respectively. These values can be considered as worst-case estimates for the uncertainty in the fitting results.

The essential information content of the PIXE-SO₄ data can be demonstrated by eliminating them from the fitting procedure. The corresponding median solutions are plotted as thick dashed lines in Fig. 2. The retrieval of total number is affected strongest at larger values of d_g because the corresponding integral is most sensitive to the information of PIXE-SO₄. The retrievals of $d_{g, \text{inv}}$, are off by up to 60% whereas the width of the distribution is overestimated by up to 140% without the mass-related information.

A first test of the algorithm with experimental data is done with average free troposphere number size distributions reported by Raes, Van Dingenen, Cuevas, Van Velthoven, and Prospero (1997) for the station Izaña, Tenerife (2360 m a.s.l.). This data set was chosen because it (a) represents an aged tropospheric aerosol under clean conditions; (b) the experimental data had been fitted with a single mode lognormal function, and (c) statistics of the fitted distributions were given (Table 1). For the given parameterized distributions CPC and impactor data were simulated by folding the size

Table 1

Modal parameters of free troposphere particle number size distributions (Raes et al., (1997), Case 1; Weingartner et al. (1999), Case 2), fitted with a single mode lognormal function based on synthetic data equivalent to those of the CARIBIC experiment for the given distribution functions

$N_{10\%}$	N	$N_{90\%}$	$d_{g,10\%}$	d_g	$d_{g,90\%}$	$\sigma_{g,10\%}$	σ_g	$\sigma_{g,90\%}$	Source
236	425	614	40	53	66	1.73	1.89	2.05	Case 1
357	422	516	26	52	87	1.24	1.85	2.51	Fitting
	345			38			2.17		Case 2, Mode 1
	143			129			1.79		Case 2, Mode 2
429	491	645	19	59	106	1.5	2.3	3.5	Fitting

$N_{10\%}$, $N_{90\%}$ refers to 10% and 90% percentiles of the fitting solutions, respectively. Diameters are given in nm, number concentrations in cm^{-3} .

distributions with the collection efficiencies of the four CARIBIC sensors. To simulate the PIXE data, we assumed all particles to consist of sulfate only. Then these simulated data were used as input to the search algorithm. Statistics of the fitting results meet the experimental central values very well and, in the case of total number, encompass the respective experimental range (Table 1). For d_g and σ_g a considerably wider range of distribution parameters than found experimentally is retrieved by the fitting procedure.

Fitting measured partial integrals of the particle size distribution with one lognormal function is a compromise based on the limited available experimental information (4 channels). In the lower troposphere it is expected to find often two, in situations with very recent nucleation, even three modes in the CARIBIC size range (Covert et al., 1996). Consequently, approximations with only one lognormal mode will be distorted representations of multimodal distributions, as indicated in the fitting results discussed below. In order to test this effect synthetic data were calculated for the bimodal average submicrometer size distribution given by Weingartner, Nyeki, and Baltensperger (1999) for the high altitude site Jungfrauoch (3580 m a.s.l.). These data were fitted with the single lognormal algorithm yielding the results compared in Table 1 with the parameters of the given bimodal distribution.

Whereas total number is preserved well by the fitting of synthetic data, the single-mode fitting broadens the distribution with a value of geometric median diameter in between those for the given bimodal distribution. It is noted, however, that large-scale aerosol models often represent the atmospheric aerosol by no more than a single lognormal distribution. Thus, monomodal fits to atmospheric aerosol data are of value in constraining large-scale models of aerosol effects.

5. Fitting results

With increasing allowances in experimental uncertainties more solutions are found by the algorithm. Proportionally, uncertainties in fitted size distributions increase, eventually to the extent of preventing meaningful interpretations of the fitting results. The following results all refer to experimental uncertainties of 20% for the CPCs and -20 – 50% for the lower and upper bounds of the PIXE-SO₄ data, respectively. Larger assumed uncertainties preserve the median solutions while increasing the corresponding 90% ranges.

Table 2

Grand average fitted modal parameters total number N , geometric median diameter d_g , and geometric standard deviation σ_g of 51 CARIBIC samples

N (cm^{-3})	d_g (nm)	σ_g	Statistical parameter
2430	17	1.4	10% percentile ^a
4280	25	1.7	Median
10800	34	2.0	90% percentile ^a

^aAll concentrations refer to STP. As percentiles the medians of the integrals calculated with 10% and 90% values of the lognormal parameters are given.

The fitted lognormal parameters for all samples are collected in Fig. 3. Table 2 gives their summary statistics. Whereas median total numbers vary by a factor of 16, fitted geometric median diameters and standard deviations are considerably more stable. Their values are within a factor of three and two, respectively. The geometric median diameters agree well with the upper tropospheric values determined by Zaizen et al. (1996).

In order to investigate latitudinal dependencies, weighted averages of fitting results were calculated with the weights being the fractions of sample times spent in 5° latitude bins between 10° and 50° north. The results are given in Fig. 4. Both primary data and fitting results show samples that are influenced by recent particle nucleation. In the primary results these are samples with highest number concentrations. Geographical aerosol distributions developed by Hermann et al. (2001a) from 41 CARIBIC flights (covering the period June 1997 to November 2000) showed frequent occurrences of particle nucleation or direct ultrafine particle emissions both near the lowest latitudes (e.g., through deep convective transport and oxidation of precursor gases) and over Europe (e.g., through aircraft emissions and convective transport of boundary layer pollutants). This latitudinal trend shows clearly in the modal parameter total number N in Fig. 4.

The latitudinal distributions of the other two lognormal parameters are quite different from that of N . Whereas the geometric median diameter decreases north of 35° the spread of the distribution increases in the same region. These opposite trends can be interpreted by a move towards more frequent recent UT/LS nucleation events that should more correctly be represented by bimodal size distributions with separate ultrafine particle modes. However, such structures cannot be resolved by the present methodology and there are no comparable data available from other experiments.

A confounding factor of all latitudinal trends is illustrated in the bottom part of Fig. 4. It depicts the bin-averaged fraction of time that each sample spends in the stratosphere. The air mass assignment was derived from concurrent CARIBIC ozone data using an ozone-based definition of the tropopause developed by Andreas Zahn (private communication). Due to the nearly constant cruising altitudes of the aircraft the probability of sampling stratospheric air naturally increases with increasing latitude. Consequently, the northernmost samples often are from a mixture of tropospheric and stratospheric air. To date only two samples were taken exclusively in the stratosphere. Thus, no statistical UT/LS segregation is possible yet.

In 18% of the samples the data of CPC1 and CPC3 differ by less than the experimental uncertainty. When excluding these samples from the fitting procedure as underdetermined data sets, neither the

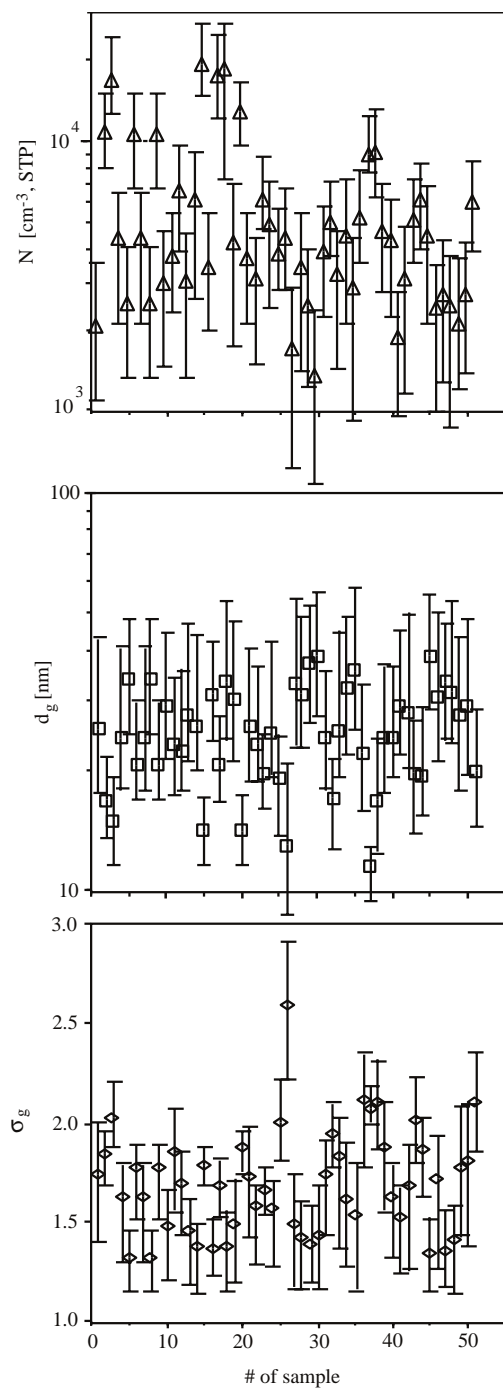


Fig. 3. Fitted lognormal parameters for the 51 CARIBIC samples. The fitted lognormal parameters N , (▲), d_g , (□), and σ_g , (◆), represent median solutions. 90% of a total of 100 solutions are found within the given error bars. All volumetric data refer to STP.

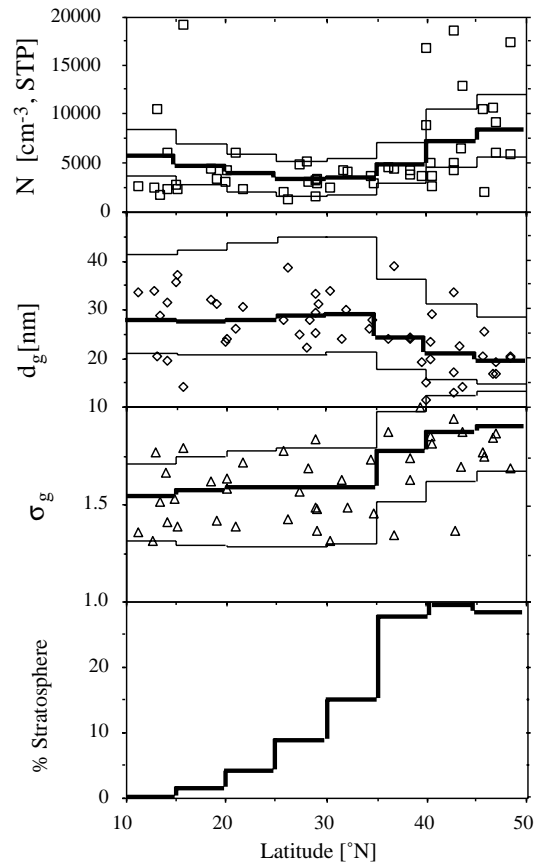


Fig. 4. Median fitted lognormal parameters N , d_g , and σ_g , averaged over 5° latitude bins. Thin lines indicate bin-averaged 10% and 90% percentiles of the respective parameters. Average fractions of the total sample time spent in the stratosphere are plotted as % stratosphere. Median fitting results for individual samples are indicated by squares for N , diamonds for d_g , and triangles for σ_g . All volumetric data refer to STP.

summary statistics nor the latitudinal distributions change significantly. We interpret this finding as support of the robustness of our overall results.

6. Conclusions

Number and mass related aerosol results from 18 long-range commercial flights of the project CARIBIC in the upper troposphere and lower stratosphere were evaluated with a new random search algorithm to derive particle size distributions. The method fits one lognormal distribution to each data set consisting of three particle number concentrations in different size ranges and one sulfur mass concentration. Through tests of the algorithm with synthetic data and size distributions from mountain stations the retrieval capabilities of the algorithm are established.

The fitting of aerosol data from 51 samples yields lognormal distribution parameters. Their latitudinal trends indicate the influence of tropical and mid-latitudinal aerosol source regions. The size distributions provide useful parameters for the validation of global aerosol models in a largely uncharted part of the atmosphere.

Acknowledgements

Matter Part of this work has been funded by the European Commission through Contract No. ENV-CT95-0006. We gratefully acknowledge the support by the carrier of the CARIBIC payload and industry partner of the project, LTU International Airways.

References

- Birmili, W., Wiedensohler, A., Heintzenberg, J., & Lehmann, K. (2001). Atmospheric particle number size distribution in Central Europe: Statistical relations to air masses and meteorology. *Journal of Geophysical Research*, in press.
- Brasseur, G., Cox, R. A., Hauglustaine, D., Isaksen, I., Lelieveld, J., Lister, D. H., Sausen, R., Schumann, U., Wahner, A., & Wiesen, P. (1998). European scientific assessment of the atmospheric effects of aircraft emissions. *Atmospheric Environment*, 32(13), 2329–2418.
- Brenninkmeijer, C. A. M., Crutzen, P. J., Fischer, H., Güsten, H., Hans, W., Heinrich, G., Heintzenberg, J., Hermann, M., Immelmann, T., Kersting, D., Maiss, M., Nolle, M., Pitscheider, A., Pohlkamp, H., Scharffe, D., Specht, K., & Wiedensohler, A. (1999). CARIBIC—civil aircraft for global measurements of trace gases and aerosols in the tropopause region. *Journal of Atmospheric and Oceanic Technology*, 16, 1373–1383.
- Brock, C. A., Hamill, P., Wilson, J. C., Jonsson, H. H., & Chan, K. R. (1995). Particle formation in the upper tropical troposphere: A Source of nuclei for the stratospheric aerosol. *Science*, 270, 1650–1653.
- Clarke, A. D. (1993). Atmospheric nuclei in the Pacific mid-troposphere: Their nature, concentration and evolution. *Journal of Geophysical Research*, 98(11), 20633–20647.
- Covert, D. S., Wiedensohler, A., Aalto, P., Heintzenberg, J., McMurry, P. H., & Leck, C. (1996). Aerosol number size distributions from 3 to 500 nm diameter in the arctic marine boundary layer during summer and autumn. *Tellus*, B48, 197–212.
- Crutzen, P. J., & Andreae, M. O. (1990). Biomass burning in the tropics: Impact on atmospheric chemistry and biogeochemical cycles. *Science*, 250, 1669–1678.
- de Reus, M., Ström, J., Kulmala, M., Pirjola, L., Lelieveld, J., Schiller, C., & Zöger, M. (1998). Airborne aerosol measurements in the tropopause region and the dependence of new particle formation on preexisting particle number concentration. *Journal of Geophysical Research*, 103(D23), 31255–31263.
- Deepak, A. (Ed.). (1977). *Inversion methods in atmospheric remote sounding*. New York: Academic Press, 622pp.
- Ferry, G. V., Pueschel, R. F., Strawa, A. W., Kondo, Y., Howard, S. D., Verma, S., Mahoney, M. J., Bui, T. P., Hannan, J. R., & Fuelberg, H. E. (1999). Effects of aircraft on aerosol abundance in the upper troposphere. *Geophysical Research Letters*, 26(15), 2399–2402.
- Hagen, D. E., Podzimek, J., & Trueblood, M. B. (1995). Upper-tropospheric aerosol sampled during Project FIRE IFO II. *Journal of Atmospheric Science*, 52(23), 4196–4209.
- Hamill, P., Jensen, E. J., Russell, P. B., & Bauman, J. J. (1997). The life cycle of stratospheric aerosol particles. *Bulletin of the American Meteorological Society*, 78(7), 1395–1410.
- Heintzenberg, J. (1975). Determination in situ of the size distribution of the atmospheric aerosol. *Journal of Aerosol Science*, 6, 291–303.
- Heintzenberg, J. (1978). Particle size distributions from scattering measurements of nonspherical particles via Mie-theory. *Contributions to Atmospheric Physics*, 51, 91–99.
- Heintzenberg, J., & Covert, D. S. (1987). Chemically resolved submicrometric size distribution and external mixing of the Arctic haze aerosols. *Tellus*, B39, 374–382.

- Hermann, M. (2000). Development and application of an aerosol measurement system for use on commercial aircraft. Ph.D. Thesis, University of Leipzig, Leipzig, 114pp.
- Hermann, M., Heintzenberg, J., Wiedensohler, A., Brenninkmeijer, C. A. M., Heinrich, G., & Zahn, A. (2001a). Meridional distributions of aerosol particle number concentrations in the upper troposphere and lower stratosphere obtained by CARIBIC flights. *Journal of Geophysical Research*, submitted for publication.
- Hermann, M., Stratmann, F., Wilck, M., & Wiedensohler, A. (2001b). Sampling characteristics of an aircraft-borne aerosol inlet system. *Journal of Atmospheric and Oceanic Technology*, 18, 7–19.
- Hermann, M., & Wiedensohler, A. (2001). Counting efficiency of condensation particle counters at low-pressures with illustrative data from the upper troposphere. *Journal of Aerosol Science*, 32, 975–991.
- Hofmann, D. (1993). Twenty years of balloon-borne tropospheric aerosol measurements at Laramie, Wyoming. *Journal of Geophysical Research*, 98(D7), 12 753–12 766.
- Ito, T. (1993). Size distribution of Antarctic submicron aerosols. *Tellus*, 45B, 145–159.
- Jaenicke, R. (1992). Vertical distribution of atmospheric aerosols. In N. Fukuta & P.E. Wagner (Eds.), *13th International Conference on Nucleation and Atmospheric Aerosol* (pp. 417–425). Deepak Publishing: Salt Lake City.
- Krieger, U. K., Mössinger, J. C., Luo, B., Weers, U., & Peter, T. (2000). Measurement of the refractive indices of H₂SO₄–HNO₃–H₂O solutions to stratospheric temperatures. *Applied Optics*, 39, 3691–3703.
- Malmqvist, K. G. (1984). Pixe—a useful tool in studies of work environment aerosols. *Nuclear Instruments and Methods*, 3, 529–540.
- Martinsson, B. G., Papaspiropoulos, G., Heintzenberg, J., & Hermann, M. (2001). Fine mode particulate sulphur in the tropopause region measured from intercontinental flights (CARIBIC). *Geophysical Research Letters*, 28(7), 1175–1178.
- Murphy, D. M., Thomson, D. S., & Mahoney, M. J. (1998). In situ measurements of organics, meteoritic material, mercury and other elements in aerosols at 5–19 km. *Science*, 282, 1664–1669.
- Papaspiropoulos, G., Mentes, B., Kristiansson, P., & Martinsson, B. G. (1999). A high sensitivity elemental analysis methodology for upper tropospheric aerosol. *Nuclear Instruments and Methods*, B 150, 356–362.
- Pueschel, R. F., Livingston, J. M., Ferry, G. V., & DeFelice, T. E. (1994). Aerosol abundances and optical characteristics in the Pacific Basin free troposphere. *Atmospheric Environment*, 28(5), 951–960.
- Puttock, J. S. (1981). Data inversion for cascade impactors: fitting sums of log-normal distributions. *Atmospheric Environment*, 15, 1709–1716.
- Raes, F., Van Dingenen, R., Cuevas, E., Van Velthoven, P. F. J., & Prospero, J. M. (1997). Observations of aerosols in the free troposphere and marine boundary layer of the subtropical Northeast Atlantic: Discussion of processes determining their size distribution. *Journal of Geophysical Research*, 102(D17), 21 315–21 328.
- Schröder, F., Brock, C. A., Baumann, R., Petzold, A., Busen, R., Schulte, P., & Fiebig, M. (2000). In-situ studies on volatile jet exhaust particle emissions—Impacts of fuel sulfur content and environmental conditions on nuclei-mode aerosols. *Journal of Great Lakes Research*, 105D, 19941–19954.
- Schröder, F., & Ström, J. (1997). Aircraft measurements of sub micrometer aerosol particles (> 7 nm) in the midlatitude free troposphere and tropopause region. *Atmospheric Research*, 44, 333–356.
- Schröder, F. P. (2000). Vertikalverteilung und Neubildungsprozesse des Aerosols und partikelförmige Flugzeugemissionen in der freien Troposphäre und Tropopausenregion. Ph.D. Thesis, Ludwig-Maximilians-Universität, München, 145pp.
- Schröder, F. P., Kärcher, B., Petzold, A., Baumann, R., Busen, R., Hoell, C., & Schumann, U. (1998). Ultrafine aerosol particles in aircraft plumes: In situ observations. *Geophysical Research Letters*, 25(15), 2789–2792.
- Sheridan, P. J., Brock, C. A., & Wilson, J. C. (1994). Aerosol particles in the upper troposphere and lower stratosphere: Elemental composition and morphology of individual particles in northern midlatitudes. *Geophysical Research Letters*, 21, 2587–2590.
- Shifrin, K. S., & Kolmakkov, I. B. (1967). Calculation of size particle spectrum by direct and integral values of small-angle scattering pattern. *Izvestiya Atmospheric and Oceanic Physics*, 3, 1271–1279.
- Ström, J., Fischer, H., Lelieveld, J., & Schröder, F. (1999). In situ measurements of microphysical properties and trace gases in two cumulonimbus anvils over western Europe. *Journal of Geophysical Research*, 104(D10), 12 221–12 226.
- Sverdrup, G. M., & Whitby, K. T. (1977). Determination of submicron atmospheric aerosol size distributions by use of continuous analog sensors. *Environmental Science and Technology*, 11(13), 1171–1176.

- Tabazadeh, A., Toon, O. B., Clegg, S. L., & Hamill, P. (1997). A new parameterization of H₂SO₄/H₂O aerosol composition: Atmospheric implications. *Geophysical Research Letters*, 24(15), 1931–1934.
- Tampieri, F., & Tomasi, C. (1976). Size distribution models of fog and cloud droplets in terms of the modified gamma function. *Tellus*, 28, 332–347.
- Wang, Y., Liu, S. C., Anderson, B. E., Kondo, Y., Gregory, G. L., Sachse, G. W., Vay, S. A., Blake, D. R., Singh, H. B., & Thompson, A. M. (2000). Evidence of convection as a major source of condensation nuclei in the northern midlatitude upper troposphere. *Geophysical Research Letters*, 27, 369–372.
- Weingartner, E., Nyeki, S., & Baltensperger, U. (1999). Seasonal and diurnal variation of aerosol size distributions ($10 < D < 750$ nm) at a high-alpine site (Jungfraujoch 3580 m a.s.l.). *Journal of Geophysical Research*, 104(D21), 26 809–26 820.
- Wright Jr., D. L. (2000). Retrieval of optical properties of atmospheric aerosols from moments of the particle size distribution. *Journal of Aerosol Science*, 31(1), 1–18.
- Yamato, M., & Ono, A. (1989). Chemical and physical properties of stratospheric aerosol particles in the vicinity of tropopause folding. *Journal of Meteorological Society of Japan*, 67, 147–165.
- Zaizen, Y., Ikegami, M., Tsutsumi, Y., Makino, Y., Okada, K., Jensen, J., & Gras, J. L. (1996). Number concentration and size distribution of the aerosol particles in the middle troposphere over the Western Pacific. *Atmospheric Environment*, 30(10/11), 1755–1762.